Applied Catalysis B: Environmental 192 (2016) 161–170

Contents lists available at ScienceDirect

Applied Catalysis B: Environmental

journal homepage: www.elsevier.com/locate/apcatb

Nano-crystalline, mesoporous aerogel sulfated zirconia as an efficient catalyst for esterification of stearic acid with methanol

K. Saravanan[a,b], Beena Tyagi[a,b,*], Hari C. Bajaj[a,b]

[a] Division of Inorganic Materials and Catalysis, Council of Scientific and Industrial Research, Central Salt and Marine Chemicals Research Institute (CSIR-CSMCRI), G.B. Marg, Bhavnagar, Gujarat 364 002, India
[b] Academy of Scientific and Innovative Research (AcSIR), CSIR-CSMCRI, G.B. Marg, Bhavnagar, Gujarat 364 002, India

ARTICLE INFO

Article history:
Received 17 December 2015
Received in revised form 4 March 2016
Accepted 16 March 2016
Available online 17 March 2016

Keywords:
Supercritical drying
Aerogel sulfated zirconia
Mesoporous solid acid catalyst
Esterification
Methyl stearate

ABSTRACT

Aerogel sulfated zirconia (A-SZr) solid acid catalyst was prepared by sol–gel method followed by supercritical drying (SCD) using *n*-propanol as alcoholic solvent. For comparison, xerogel sulfated zirconia (X-SZr) was also prepared by sol–gel followed by conventional thermal drying method. A-SZr catalyst has lower nano-crystallite size, higher BET surface area, pore volume and ordered mesoporous structure with complete absence of micropores along with more number of scattered and accessible Brönsted and Lewis acid sites as compared to X-SZr. The evaluation of its catalytic performance for esterification of stearic acid with methanol exhibited 88% yield of methyl stearate at 60 °C after 7 h. A-SZr catalyst showed significant higher reaction rate (18.94 mmol h^{-1} g^{-1}) and TOF (8.55 h^{-1}) than X-SZr (12.94 mmol h^{-1} g^{-1} and 3.92 h^{-1}, respectively). A-SZr catalyst also exhibited higher activity than other heterogeneous acid catalysts such as ion-exchange resins, Nafion and acid clay under the similar reaction conditions; as well as it showed comparable activity with conventional Brönsted (H_2SO_4) and Lewis ($ZrOCl_2$) acids indicating its potential to replace the homogeneous acid catalysts.

1. Introduction

The fatty acid methyl esters (FAMEs) are synthesized either from the esterification of fatty acids in presence of conventional homogenous acid (e.g. H_2SO_4, HF, *p*-TSA) catalysts or by the transesterification of vegetable oils and animal fats using basic (e.g. KOH/NaOH) catalysts; the latter route is the conventional industrial method of producing FAMEs, to be used as biodiesel [1]. The presence of a significant amount of free fatty acids (FFAs) in the low-cost oils such as non-edible oils or waste cooking oils needs esterification as an essential step before transesterification to avoid the soap formation with liquid basic catalyst [2,3]. Moreover, fatty acids are the by-products of the food processing in oleochemical industry, e.g. 4–8% of FFAs of total crude palm oil is produced in the physical refining [4]. The use of these FFAs as raw material for the synthesis of FAMEs is beneficial from economical and industrial point of view. Therefore, acid catalyzed esterification of long-alkyl chain fatty acids has recently received much attention [5]. Stearic acid ($C_{18}H_{36}O_2$, *n*-octadecanoic acid) is one of the saturated fatty acid present in edible (1–5%), non-edible oils (1–9%) [6], waste greases (13%) and beef tallow (15%) [5]. It is mainly produced by the oleochemical (palm oil) industry and has been the primary fatty acid product in Malaysia [7]. Alkyl stearate of short chain alcohols namely methanol, ethanol, propanol and butanol are used as solvent, softening agent in polymers, textile and cosmetic industry and are one of the important component of FAMEs to be used as renewable fuel (biodiesel) [8]. Methyl stearate is also used as a nonionic surfactant to solubilize a variety of chemical species by dissociating aggregates and unfolding proteins [9].

The increasing environment and energy concerns have prompted an extensive demand to replace the conventional homogenous acid catalysts due to their disadvantages of corrosiveness, non-separatibility, non-reusability, high activity causing formation of side-products and post-treatment process resulting in large salt generation and loss of required yield. Therefore, search for the alternative eco-friendly heterogeneous acid catalysts that can be easily separable, re-usable and reduce production cost has emerged [5,10–12]. A number of solid acid catalysts have been studied for the esterification of various saturated and unsaturated fatty acids [5,10–12]; however, esterification of stearic acid has not been studied much; only few studies over acid activated clay [8,13,14], acidic resin [15] and silica supported tungstophosphoric acid [16] are reported, which showed a varied range of reaction variables such as acid to alcohol ratio (1:11–1:175), temperature (78–160 °C)

* Corresponding author.
E-mail address: btyagi@csmcri.org (B. Tyagi).

http://dx.doi.org/10.1016/j.apcatb.2016.03.037
0926-3373/

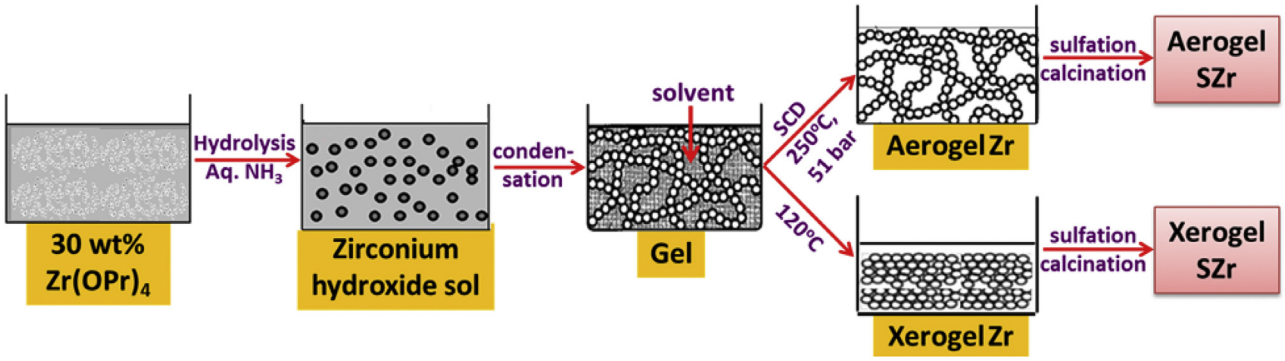

Scheme 1. Synthesis of aerogel and xerogel SZr via sol-gel followed by supercritical drying (SCD) and thermal drying technique, respectively.

and catalyst amount (9–20 wt%) [8,13–16] to achieve good activity. The higher reaction temperature, higher amount of alcohol and catalyst are not desired from energy and economic point of view.

Sulfated zirconia (SZr) has become one of the most widely studied solid acid catalysts [17] after showing potential activity for alkane isomerization at mild temperature [18] due to its strong acidity. It is a unique acid catalyst having both Brönsted as well as Lewis acidity due to the electron withdrawing effect of sulfate groups bonded to zirconia surface. Kiss et al. [19] found SZr as the most promising catalyst among various solid acids including zeolites, ion exchange resins and sulfated metal oxides such as titania and tin oxide for the esterification of lauric acid with various alcohols. SZr showed excellent activity for esterification of various saturated/unsaturated fatty acids [20–23] and also for simultaneous esterification and transesterification of oils having high amount of free fatty acid contents [24,25]; however, there is no report for its use for esterification of stearic acid. Moreover, the catalytic properties of SZr strongly depend on its structural, textural and acidic properties which in turn significantly influenced by the method employed for its synthesis [26]. In our recent studies, we have prepared SZr catalyst by sol-gel, [27a,b] conventional precipitation [27c,d] and template assisted [27e] techniques, which showed excellent activity for the esterification of C8, C14 and C16 fatty acids with methanol and other short chain alcohols.

In the present study, we report the esterification of stearic acid with methanol over nano-crystalline, mesoporous aerogel SZr catalyst (A-SZr) with a view to combine the advantage of higher surface area and pore volume for easy diffusion pathways of longer alkyl chain of fatty acid and ester molecules along the nanoporous structure and availability of more number of accessible active acid sites at higher surface area. A-SZr was prepared by sol–gel method followed by supercritical drying of gel using *n*-propanol as alcoholic solvent. The various reaction variables have been optimized to achieve maximum yield of methyl stearate. The comparison of catalytic activity of aerogel SZr (dried under supercritical conditions) with xerogel SZr catalyst (dried under conventional thermal heating) and other heterogeneous as well as homogeneous catalysts has clearly demonstrated the better performance of aerogel SZr catalyst thus giving an insight about the significant influence of higher mesoporosity, surface area and Brönsted acidity for the studied reaction. To the best of our knowledge, no study has been reported for the esterification of stearic acid with methanol over aerogel SZr solid acid catalyst so far.

2. Experimental

2.1. Materials

Zirconium *n*-propoxide [$Zr(OPr)_4$] (70 wt% in *n*-propanol) was procured from Sigma-Aldrich, Germany. *n*-propanol (99%) was obtained from s. d. fine-chem. Ltd, India and aqueous ammonia solution (25%) and sulfuric acid (98%) was from Rankem, India. Stearic acid (99%) and dried methanol (99.8%) were bought from SRL Pvt. Ltd, India. All the chemicals were used as such.

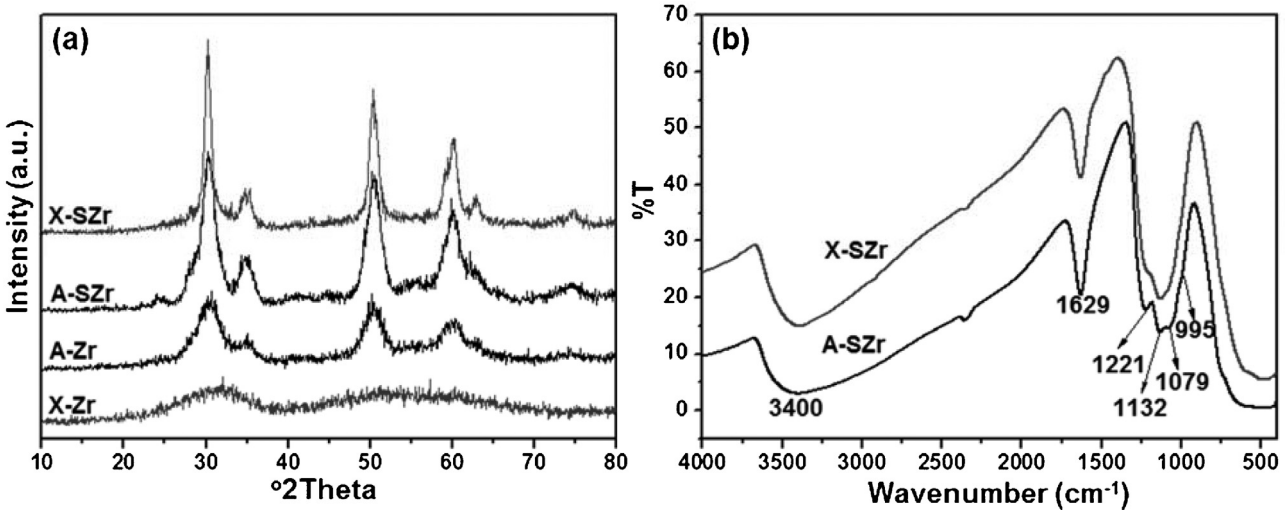

Fig. 1. (a) PXRD pattern of X-Zr, A-Zr, A-SZr and X-SZr and (b) FT-IR spectrum of A-SZr and X-SZr catalysts.

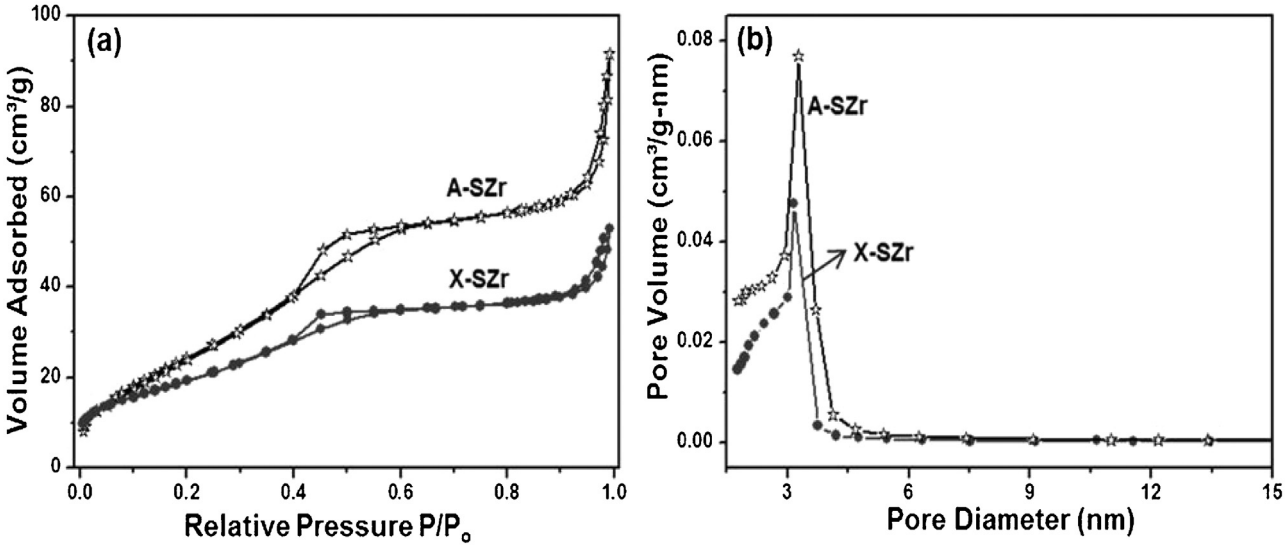

Fig. 2. (a) N_2-adsorption-desorption isotherms and (b) pore size distribution of A-SZr and X-SZr catalysts.

2.2. Catalyst synthesis

2.2.1. Synthesis of aerogel zirconia (A-Zr) via supercritical drying (SCD)

Aerogel zirconia was prepared by sol-gel method followed by supercritical drying using *n*-propanol [28a] followed by sulfation and calcination (Scheme 1). In a typical synthesis procedure, zirconium *n*-propoxide (70 wt%, 35 g) diluted to 30 wt% with *n*-propanol was hydrolyzed by dropwise addition of aqueous NH_3 under continuous magnetic stirring till the pH reaches ~10. After hydrolysis, the sol was continuously stirred for 3 h at ambient temperature to polymerize the gel. The three-dimensional network of zirconia gel has water and *n*-propanol molecules as solvent, formed during the condensation and polymerization steps of sol-gel process, within its porous structure. The wet gel samples obtained above were initially washed 4–5 times with *n*-propanol to remove water molecules, as water have detrimental effect upon the textural properties of the aerogels due to its higher critical temperature (374 °C) and pressure (~222 bar).

The evacuation of the solvent from the pores of zirconia gel was carried out under supercritical conditions of temperature (250 °C) and pressure (51 bar) of *n*-propanol in a high pressure autoclave reactor (Autoclave Engineers, USA, model E 01055 A). In a typical drying process, the washed gel obtained above was placed in an autoclave which was initially flushed with nitrogen followed by raising the pressure and temperature above the critical point of *n*-propanol. After a period of thermal equilibration (1 h), the pressure was isothermally released at a constant rate to remove residual alcohol and subsequently cooled to room temperature. The white fine light powder of aerogel zirconia (A-Zr) was obtained.

2.2.2. Synthesis of xerogel zirconia (X-Zr) via conventional thermal drying

For comparison, xerogel zirconia sample was also prepared with above described synthetic procedure followed by conventional thermal drying of zirconia gel (Scheme 1) in an oven at 120 °C temperature for 12 h [28b].

2.2.3. Synthesis of sulfated zirconia

Both aerogel and xerogel zirconia samples were treated with 1 N H_2SO_4 (15 ml/g) for 30 min under stirring followed by filtration, drying at 120 °C for overnight and calcination at 600 °C for 4 h under static air. The samples were designated as A-SZr and X-SZr for aerogel and xerogel sulfated zirconia catalysts, respectively.

2.3. Catalyst characterization

The crystallinity and the crystalline phase of A-Zr after SCD; A-SZr and X-SZr catalysts after calcination at 600 °C was determined by X-ray powder diffractometer (Philips X'pert, The Netherlands)

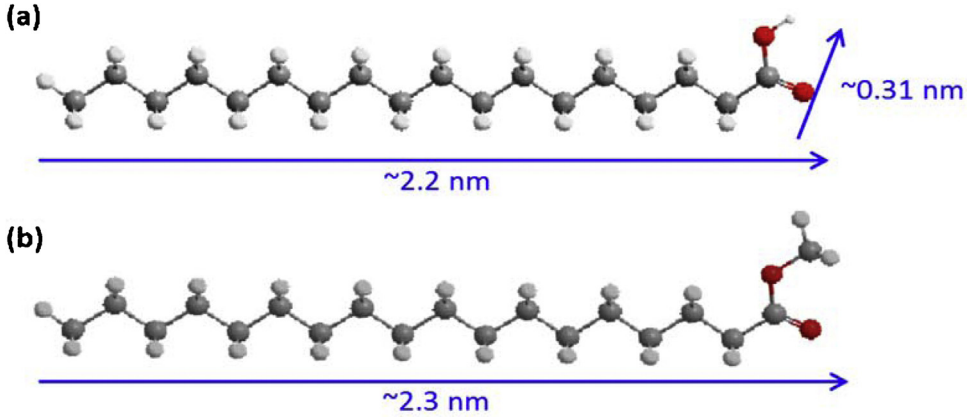

Scheme 2. Molecular size of (a) stearic acid (l = ~2.2 nm, w = ~0.31 nm) and (b) methyl stearate (l = ~2.3 nm, w = ~0.31 nm) by Gaussian software.

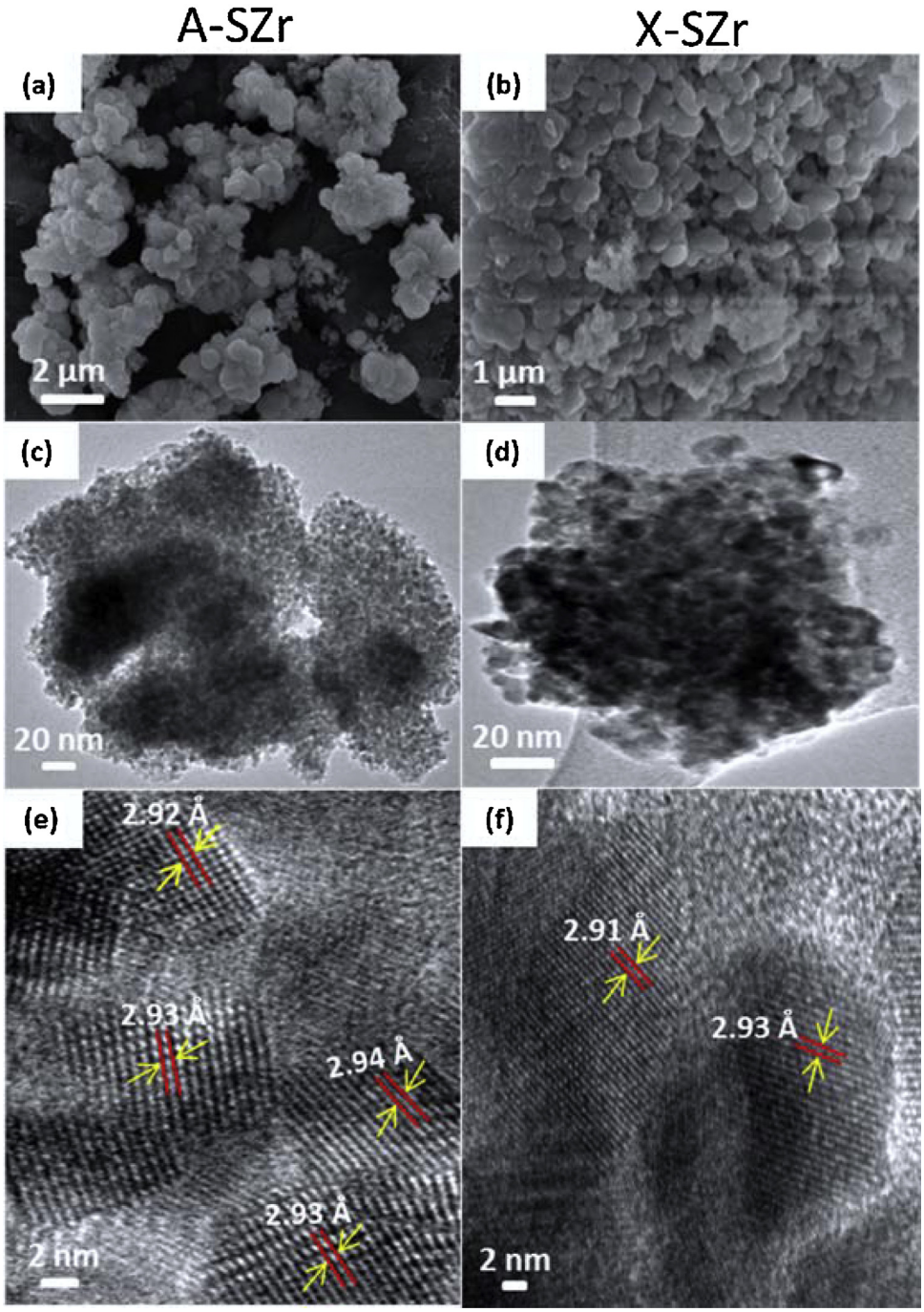

Fig. 3. (a,b) SEM (c,d) TEM and (e,f) HR-TEM images of A-SZr and X-SZr catalysts [ordered porous network structure and lattice fringes (shown by arrow)].

using CuKα radiation (λ = 1.54059 Å). The crystallite size was determined from the characteristic peak of tetragonal phase of zirconia (°2θ = 30.3) using Scherrer formula. FT-IR spectrum of A-SZr and X-SZr catalysts were recorded by FT-IR spectrophotometer (Perkin Elmer, GX, USA) in the range of 400–4000 cm^{-1} with a resolution of 4 cm^{-1} as KBr pellets. The bulk sulfur (wt%) before calcination and retained after calcination at 600 °C in both A-SZr and X-SZr catalysts were analyzed by elemental analyzer (PerkinElmer 2400, USA).

Specific BET surface area, pore volume and pore size distribution of the catalysts were determined from N_2 sorption isotherms at −196 °C (ASAP 2010, Micromeritics, USA). Surface area and pore size was calculated by BET (Brunauer–Emmett–Teller) equation and BJH (Barrett–Joyner–Halenda) method, respectively. The catalyst was degassed under vacuum (1×10^{-3} mmHg) at 150 °C for 4 h, prior to adsorption measurement to evacuate the physisorbed moisture.

The total surface acidity of A-SZr and X-SZr catalysts were measured in the temperature range of 50–900 °C by temperature programmed desorption (TPD) of NH_3 (Micromeritics Pulse Chemisorb 2720) by standard procedure [27e]. Vapor phase cyclohexanol dehydration to cyclohexene in a fixed bed reactor was used as a model reaction to assess the Brönsted acidity of A-SZr catalyst [27e].

Brönsted (B) and Lewis (L) acid sites were differentiated using pyridine as a probe by FT-IR spectrophotometer (Perkin Elmer, GX, USA) equipped with Diffuse Reflectance FT-IR (DRIFT) acces-

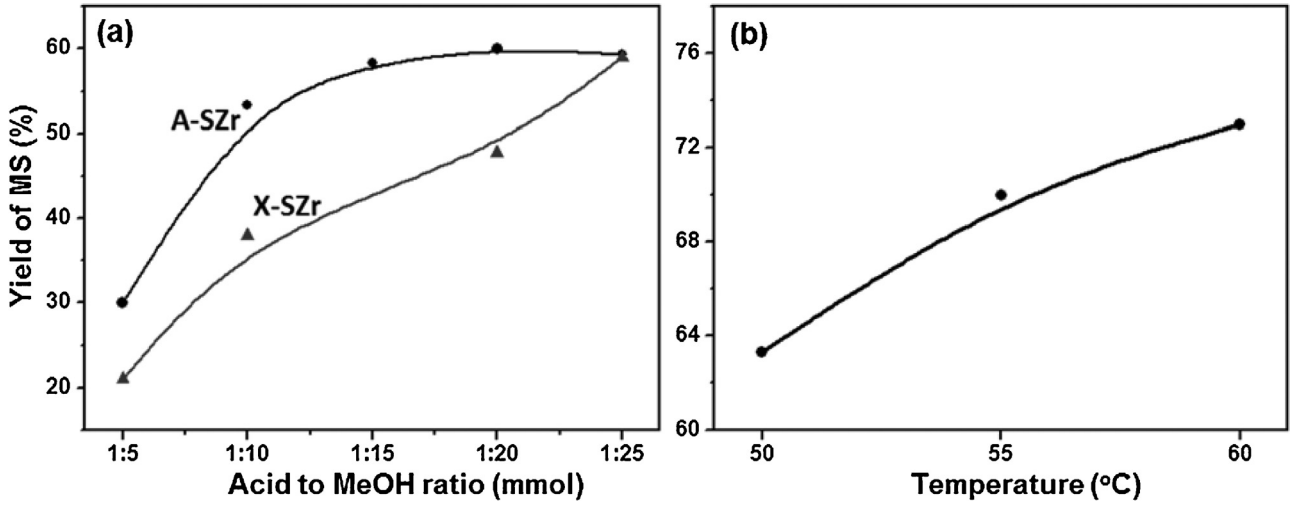

Fig. 4. Yield of methyl stearate (MS) at varied (a) acid to methanol molar ratio and (b) temperature. *Reaction conditions*: Stearic acid = 3 mmol; time = 7 h (a) temperature = 60 °C; catalyst = 1 wt%; (b) MeOH = 60 mmol; catalyst = 3 wt%.

sory (Graseby Specac, P/N 19900) and an automatic temperature controller (Graseby Specac, P/N 20130) [27e]. The quantification of B and L acid sites concentration and B/L ratio was done from the characteristic peak area measured at 150 °C by molar extinction coefficient method (using ϵ_B = 1.67 cm/μmol and ϵ_L = 2.22 cm/μmol) [30,31] as described in earlier report [27e].

The microscopic study of both A-SZr and X-SZr catalysts were done with a scanning electron microscope (SEM) (Leo series VP1430, Germany) having a silicon detector under a pressure of $>1.34 \times 10^{-2}$ Pa. The catalysts were dispersed in ethanol by sonication and coated with gold using a Polaron Sputter Coater. TEM micrograph was obtained with a transmission electron microscope (JEOL JEM 2100) by dispersing the A-SZr and X-SZr catalysts in ethanol by sonication and deposited on a Cu grid coated with carbon film.

Particle size of A-SZr and X-SZr catalysts were obtained by particle size analyzer, Spectro SizeTM 300 (NaBiTec, Germany) after dispersing a small amount of catalyst (~1 mg) in methanol (50 ml) under sonication for 40 min.

2.4. Esterification of stearic acid with methanol

In a typical liquid phase batch reaction, stearic acid (0.85 g, 3 mmol), dried methanol (1.96 g, 60 mmol) and required amount of catalyst were taken in a round bottom flask and the reactant mixture was magnetically stirred (700 rpm) in oil bath maintaining 60 °C temperature (±1 °C) for 7 h. The catalyst was separated from the reaction mixture by centrifugation and removal of methanol was done by rotatory evaporator. The yield of methyl stearate was determined by ^{1}H NMR using chloroform-*d* (99.8% atom, Sigma-Aldrich) as a solvent. The areas of the signals of methylene hydrogen, α to the carbonyl group, at 2.26–2.38 ppm (A_{CH2}) and methoxy hydrogen (CH_3O—) at 3.66 ppm (A_{ME}) were integrated to calculate the yield (%) of methyl stearate by using the following equation [32]:

$$\text{Yield(\%)ofmethylstearate} = 100 \times (2A_{ME}/3A_{CH2})$$

The acid base titration with 0.1 N alcoholic KOH using phenolphthalein indicator has also been done with time to estimate the conversion of stearic acid on the basis of acid value.

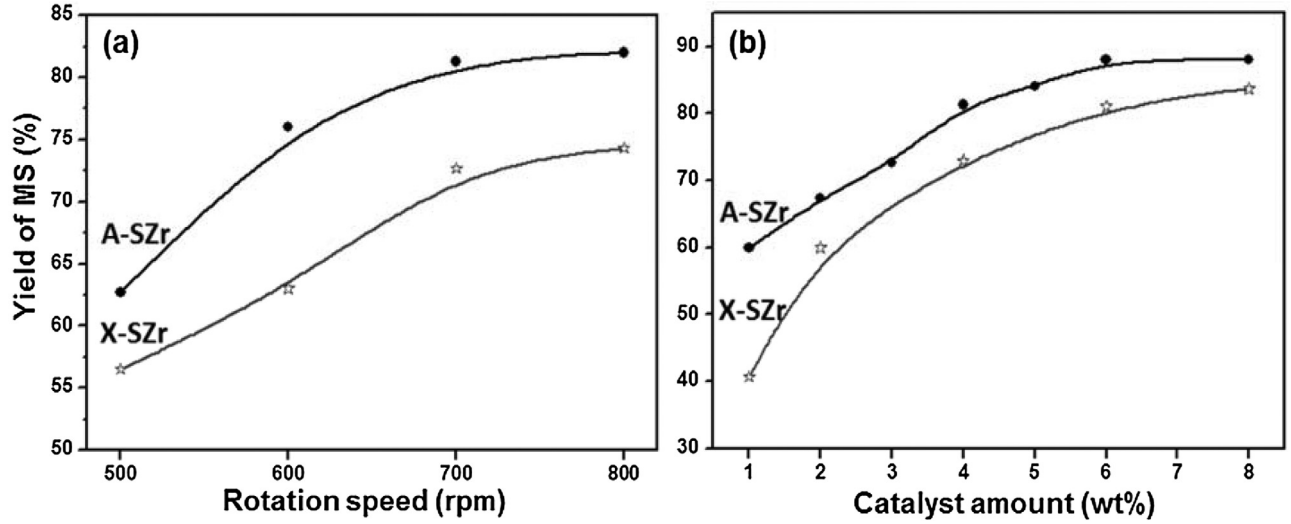

Fig. 5. Yield of methyl stearate (MS) at varied (a) stirring speed and (b) catalyst amount. *Reaction conditions*: Stearic acid = 3 mmol and MeOH = 60 mmol; time = 7 h; temperature = 60 °C. (a) catalyst = 4 wt%.

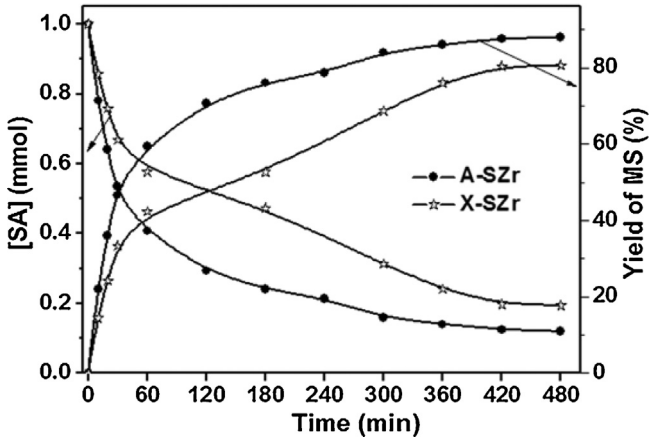

Fig. 6. Reaction profile for esterification of stearic acid (SA) with time over aerogel and xerogel SZr. *Reaction conditions*: Stearic acid = 3 mmol and MeOH = 60 mmol; catalyst = 6 wt%; temperature = 60 °C.

The reusability of A-SZr catalyst was examined by carrying out successive reaction cycles. After completing the reaction, the catalyst was separated from the reaction mixture by centrifugation, washed by ~1:1 v/v methanol:hexane (~15–20 ml in each time) mixture under ~2–3 min sonication to remove the adhered reactant and product molecules from the catalyst surface. The above obtained catalyst was dried at 120 °C for 12 h followed by activation at 600 °C for 2 h under air, before starting a new reaction cycle with fresh reactants.

3. Results and discussion

3.1. Catalysts characterization

Powder X-ray diffraction (PXRD) pattern of aerogel zirconia (A-Zr) after SCD (Fig. 1a) showed crystalline nature having predominately tetragonal crystalline phase of zirconia (°2θ = 30.3, 35.0, 50.4, 60.0). The obtained crystallinity of zirconia before calcination reflects that high pressure and temperature inside the autoclave during the SCD conditions enhanced the crystallization of the aerogels particles [28,33]. Similar observations were reported by others also [34]. On the other hand xerogel zirconia (X-Zr) after conventional thermal drying at 120 °C for 12 h showed amorphous nature (Fig. 1a).

Table 1
Physico-chemical characterization of A-SZr and X-SZr catalysts.

Catalysts	A-SZr	X-SZr
Crystallite size (nm)	5.8[a] (5.5[b])	12[a] (10[b])
Sulfur (wt%)	3.6[c] (2.0[d])	4.7[c] (2.1[d])
BET surface area (m^2/g)	142	71
Average pore volume (cm^3/g)	0.15	0.065
Micropore volume (cm^3/g)	nil	0.0031
BJH pore diameter (nm)	4.5	4.0
Total acid sites (mmol/g)	1.36	0.85
Acid site density (mmol/m^2)	0.0096	0.032
Brönsted acid sites (mmol/g)[e]	0.090	0.073
Lewis acid sites (mmol/g)[e]	0.062	0.051
Cyclohexanol dehydration	95	–

[a] By Scherrer formula in PXRD.
[b] By HR-TEM.
[c] Before calcination.
[d] After calcination.
[e] B and L = Brönsted and Lewis acid sites at 150 °C calculated by molar extinction coefficient method.

PXRD pattern of A-SZr catalyst after calcination at 600 °C showed higher crystallinity having predominately tetragonal crystalline phase (Fig. 1a). The crystallite size calculated from the characteristic tetragonal peak (°2θ = 30.3) was 5.8 nm (Table 1). X-SZr catalyst also showed tetragonal crystalline phase (°2θ = 30.2, 35.0, 50.6, 60.3) with crystallite size of 12 nm after calcination at 600 °C (Fig. 1a).

It is worth to note that SCD method resulted in smaller crystallite size (5.8 nm, ~half) as compared to conventional thermal drying, either SZr was prepared by sol-gel [present results (12 nm), 28b (11–16 nm)] or conventional method [27c,d] [(11–12 nm)]; even it was smaller than CTAB (cetyltrimethyl ammonium bromide) template assisted technique [27e (~8–9 nm)]. In SCD method, density of the gas phase becomes equal to the liquid phase at supercritical temperature and pressure that prevents the agglomerization of zirconia particles and thus resulting into the formation of nanomaterial [28a].

FT-IR spectrum of A-SZr catalyst exhibited the presence of sulfate bands at 1221, 1132, 1079 and 995 cm^{-1} (Fig. 1b), characteristic of inorganic chelating bidentate sulfate which are assigned to asymmetric and symmetric stretching frequencies of S···O and S—O bonds with C_{2v} symmetry and ν_3 and ν_1 stretching mode of SO_4^{2-} groups [35]. X-SZr catalyst also showed the sulfate peaks in the range of 990–1225 cm^{-1} (Fig. 1b). The absence of covalent S═O band at ~1400 cm^{-1} indicated the partial ionic nature and hydrated state of sulfate groups at the surface of zirconia, confirmed by the presence of a broad band at 3400 cm^{-1} for surface

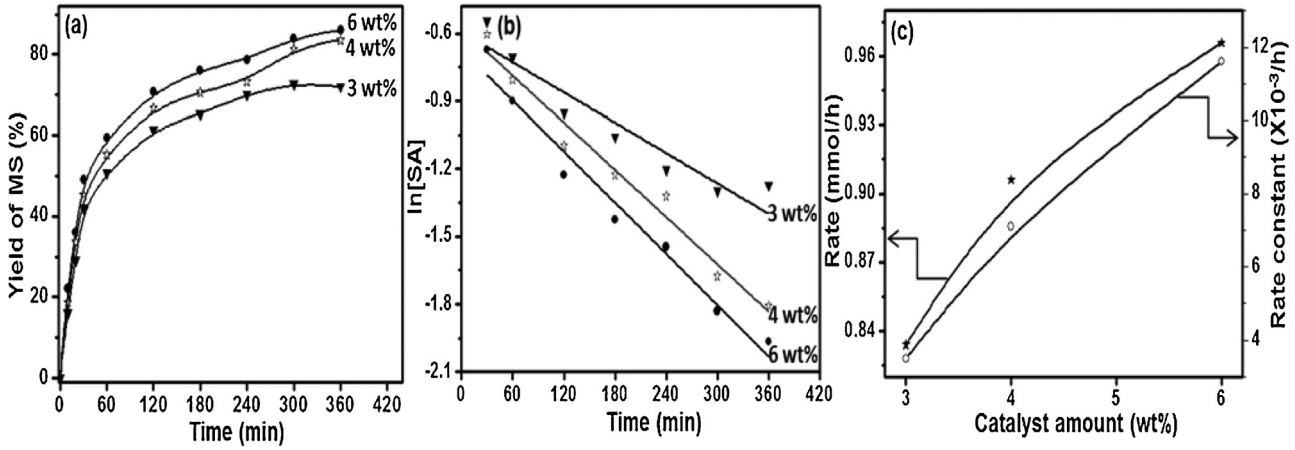

Fig. 7. Esterification of stearic acid (SA) with methanol over varied A-SZr catalyst amount (a) yield of methyl stearate (MS) (b) plot of ln[SA] versus time (c) rate of reaction and rate constant.

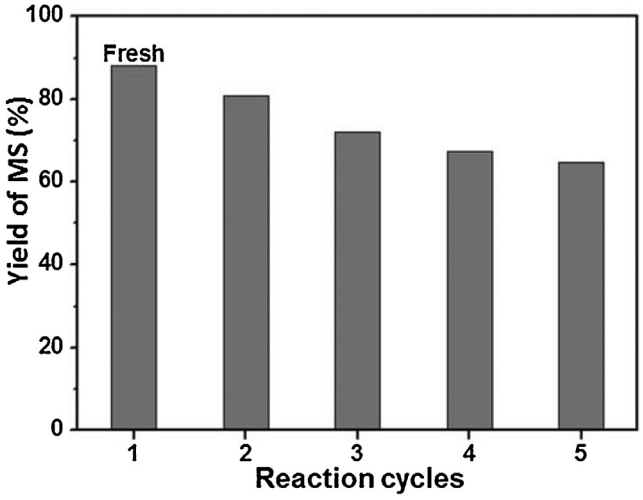

Fig. 8. Re-cyclability of A-SZr catalyst for esterification of stearic acid with methanol. *Reaction conditions*: acid to MeOH molar ratio = 1:20; catalyst = 6 wt%; temperature = 60 °C; time = 7 h.

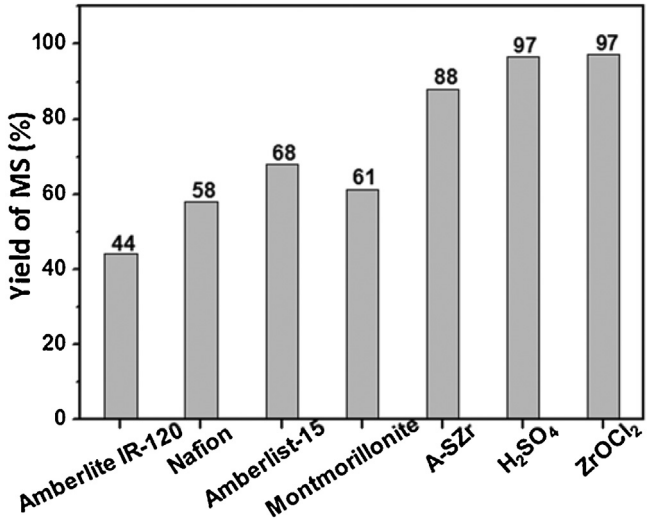

Fig. 9. Esterification of stearic acid with methanol over various heterogeneous and homogeneous acid catalysts. *Reaction conditions*: acid = 3 mmol and MeOH = 60 mmol; temperature = 60 °C; time = 7 h; catalyst = 6 wt%.

acidic hydroxyl groups showing H-bonding for ν_{OH} and an intense band at 1629 cm^{-1} for δ_{OH} associated with sulfate groups as well as zirconia surface that are responsible for the Brönsted acidity of SZr catalyst.

The bulk sulfur content in A-SZr catalyst, before and after calcination at 600 °C, was 3.6 and 2.0 wt%, respectively (Table 1). The sulfur content of X-SZr catalyst, before calcination, was higher (4.7 wt%) than A-SZr due to amorphous nature, however after calcination it was similar (2.1 wt%) (Table 1).

N_2 sorption isotherm of both A-SZr and X-SZr catalysts showed a well-defined type IV isotherm of mesoporous materials (Fig. 2a) with H2 hysteresis loop at 0.4 to ~0.6 relative pressures [36]. *t*-plot analysis of A-SZr catalyst showed the complete absence of micropores, though small amount (0.0031 cm^3/g) of micropores were present in X-SZr catalyst (Table 1). In general, conventional oven drying results in the formation of micro- as well as mesopores due to uneven heat transfer in the bulk and surface of the material; however, during SCD, the material remains under uniform temperature and pressure at supercritical point thus eliminating the liquid–vapour interface leading to the formation of mesoporous material. The BET surface area and pore volume of A-SZr was 142 m^2/g and 0.15 cm^3/g respectively, which was significantly higher than X-SZr having lower BET surface area (71 m^2/g) and pore volume (0.07 cm^3/g) (Table 1). Both catalysts are having average pore diameter of 4.0–4.5 nm with a narrow pore size distribution with mesoporous nature (Fig. 2b).

The above results clearly revealed the effect of SCD on the structural and textural properties of the catalyst in terms of nanocrystallite size and higher BET surface area and pore volume leading

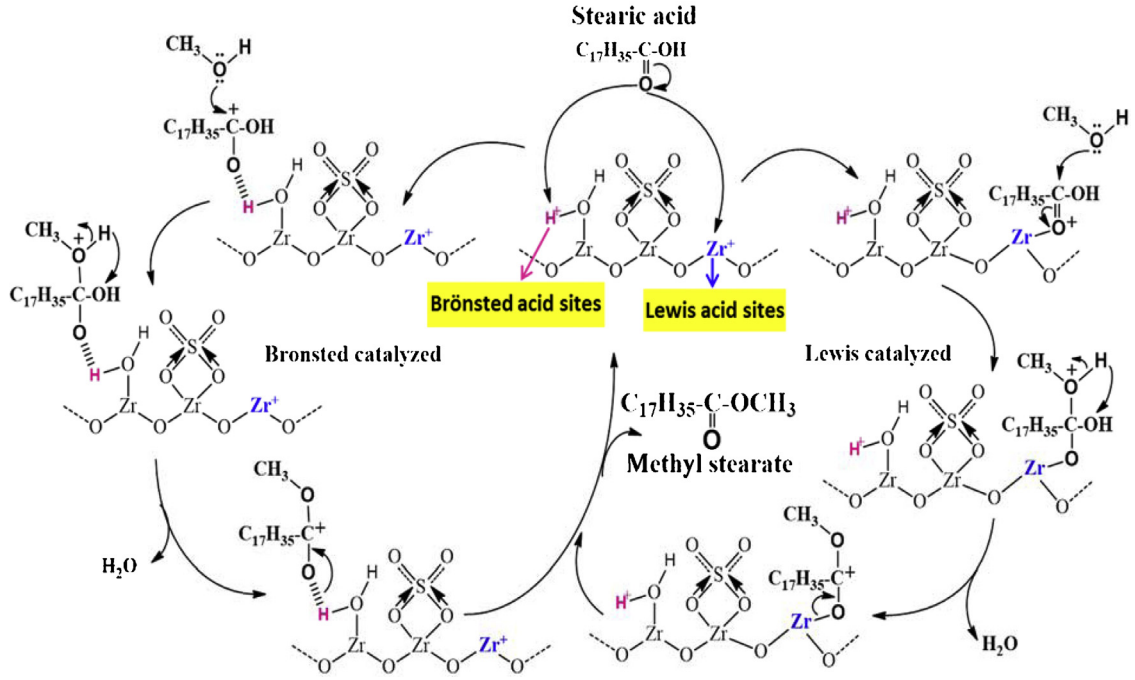

Scheme 3. Plausible structure of SZr catalyst and mechanistic representation of esterification of stearic acid with methanol to synthesize methyl stearate using Brönsted (left side) and Lewis (right side) acid sites of SZr catalyst.

to higher surface to volume ratio and facile flow of catalytic reaction.

SEM images of A-SZr showed small agglomerated spherical-shaped particles (Fig. 3a), whereas, X-SZr showed agglomerated mass of spherical particles (Fig. 3b). TEM micrograph of A-SZr catalyst showed 'worm-type' morphology (Fig. 3c), whereas X-SZr catalyst was found to have aggregates of zirconia particles (Fig. 3d). The HR-TEM image of A-SZr clearly illustrated ordered porous structure having regular lattice fringes parallel to each other forming a lamellar structure along with an ordered porous network structure (Fig. 3e). The width (~2.93 Å) between two lattice fringes of the lamellar structure as well as of network structure of A-SZr was agreed with *d*-spacing (2.92 Å) of characteristic peak of tetragonal (111) zirconia (°2θ = 30.3) calculated by PXRD. The HR-TEM image of X-SZr (Fig. 3f) also exhibited lattice fringes (~2.91 Å) of the lamellar structure agreeing with *d*-spacing (2.95 Å) of characteristic peak of tetragonal zirconia (°2θ = 30.2) calculated by PXRD. The crystallite size measured from HR-TEM images was 5.5 and ~10 nm for A-SZr and X-SZr, respectively, and was in close agreement with PXRD analysis.

The particle size analysis of A-SZr catalyst displayed the small aggregates of varying particle size in the range of 44–120 nm; some particles were of ~10–20 nm size (Fig. S1a). On the other hand, particle size of X-SZr catalyst indicated that most of the particles were of ~352 nm size (Fig. S1b). Few particles were also found to have ~24 nm. These results were also in accordance with SEM images where A-SZr showed small agglomerated particles and X-SZr showed agglomerated mass of spherical particles.

The total surface acidity of A-SZr catalyst analyzed by NH_3-TPD was 1.36 mmol/g (Table 1). NH_3-desorption peaks showed the presence of weak (102 °C), moderate to strong (554 °C) and very strong (777 °C) acid sites (Fig. S2a). The total acid sites of X-SZr catalyst was lower (0.85 mmol/g) though having weak (71 °C), moderate to strong (675 °C) and very strong (700–792 °C) acid sites (Fig. S2b). The results clearly showed that presence of same sulfur amount may result in varied number and strength of acid sites depending on the availability of surface hydroxyl and zirconia ions which in turn influenced by the synthetic protocol.

The DRIFT spectra of pyridine adsorbed A-SZr and X-SZr catalysts exhibited the characteristic peaks for pyridinium ion (Brönsted acid sites) at 1542–1545 cm^{-1} and covalently bonded pyridine (Lewis acid sites) in the range of 1441 cm^{-1} (Fig. S3). The peak at ~1490 cm^{-1} represented the combined Brönsted and Lewis acid sites. The co-existence of another Lewis and Brönsted acid sites was also evident by the peaks at ~1612 and 1636 cm^{-1} respectively. Brönsted acid sites were observed to be strong enough in both catalysts as they were present even after heating at 450 °C; though the intensity of the peaks was decreased after successive heating from 150 to 450 °C. The calculated Brönsted (B) and Lewis (L) acid site concentration at 150 °C was higher in A-SZr catalyst (0.090 and 0.062 mmol/g, respectively) as compared to X-SZr catalyst (0.073 and 0.051 mmol/g, respectively). (Table 1). The results clearly showed the presence of more number of acid sites on larger surface area in A-SZr. The lower acid site density (0.0096 mmol/m^2), i.e., total acid sites scattered on larger surface area in A-SZr generated more number of accessible B and L acid sites, compared to higher acid site density (0.032 mmol/m^2) densely distributed on smaller surface area in X-SZr.

The Brönsted acidity of A-SZr catalyst was further confirmed by evaluating its activity for a model reaction of catalytic dehydration of cyclohexanol, which showed 95% conversion of cyclohexanol (Table 1) with 100% selectivity for cyclohexene. The results indicated the presence of substantial Brönsted acidity in A-SZr catalyst and confirmed the DRIFT results.

3.2. Esterification of stearic acid with methanol

The effect of various reaction parameters such as acid to methanol molar ratio, temperature, catalyst amount, stirring speed and time has been studied to optimize the reaction variables for achieving maximum yield of selectively formed (confirmed by GC–MS analysis) methyl stearate calculated by ^{1}H NMR spectroscopy.

3.2.1. Effect of acid to methanol ratio

The reaction was studied with an acid to methanol molar ratio of 1:5 to 1:25 over 1 wt% (with respect to acid) catalyst amount at 60 °C for 7 h (Fig. 4a). The results showed 30% yield of methyl stearate with acid to methanol molar ratio of 1:5, which enhanced to 60% with successive increase in acid to methanol ratio to 1:20. However, further increasing the acid to methanol ratio to 1:25, almost similar yield of methyl stearate (59%) was observed. Hence, acid to methanol ratio of 1:20 was chosen for further study.

A comparison of activity with X-SZr catalyst under varied acid to methanol ratio was also done. The results showed that both SZr catalysts exhibited maximum ~59-60% yield of methyl stearate at acid to methanol ratio of 1:25 after 7 h; however, A-SZr catalyst displayed significant higher yield of methyl stearate at acid to methanol ratio from 1:5 to 1:20, and for X-SZr catalyst a higher acid to methanol ratio of 1:25 was required to obtain similar yield of methyl stearate (59%). The higher surface to volume ratio due to nano-crystallite size, higher BET surface area, pore volume along with relatively higher Brönsted acidity of A-SZr as compared to X-SZr catalyst resulted into higher activity for the studied reaction at acid to methanol ratio of 1:20.

An excess of alcohol may lead to dehydration or etherification in the presence of strong acid catalyst such as sulfated zirconia. No such dehydrated or ether product was detected by GC–MS analysis under the reaction conditions studied.

The yield of methyl stearate calculated by ^{1}H NMR was found almost similar to the conversion of stearic acid calculated on the basis of acid value using acid base titration.

3.2.2. Effect of reaction temperature

The effect of reaction temperature was studied in the temperature range from 50 to 60 °C (Fig. 4b). A gradual increase in the yield of methyl stearate was observed from 63 to 73% over 3 wt% catalyst amount by increasing the temperature from 50 to 60 °C after 7 h. The better solubility and miscibility of stearic acid with methanol at higher temperature (insoluble at room temperature and partially soluble at 50 °C) facilitated the protonation of the carbonyl group of stearic acid and nucleophilic attack of methanol on the acid resulting in increased yield of product. As boiling point of methanol is ~64 °C, we have studied all reactions at 60 °C to avoid any vapor loss during liquid phase batch reaction.

3.2.3. Effect of stirring speed and catalyst amount

To study the effect of mass transfer, the catalytic experiments were conducted at different stirring speeds (500 to 800 rpm) (Fig. 5a). The methyl stearate yield was lower (63%) at 500 rpm, which continuously increased till 700 rpm (81%) and no significant increase was observed by further increasing the speed to 800 rpm. Similar trend has been observed in X-SZr catalyst with lower yield of methyl stearate (67–84%) (Fig. 5a). These results indicated the absence of external mass transfer resistance at >600 rpm and the reactions were in kinetic regime, therefore further experiments were performed at a constant stirring speed of 700 rpm. Furthermore, both catalysts having mesopores of pore diameter (4.0–4.5 nm) along with particle size (120–352 nm) far greater than the molecular size of stearic acid (~2.2 nm) and methyl stearate

(~2.3 nm) (derived by Gaussian software as shown in Scheme 2) also showed the absence of internal mass transfer resistance.

A-SZr catalyst showed a linear increase in the yield of methyl stearate (60 to 88%) by increasing the catalyst amount from 1 to 6 wt% (Fig. 5b), as higher amount of acid sites is required to achieve maximum conversion of fatty acid of larger carbon chain length. However, further amount of increased acid sites in terms of catalyst amount (6–8 wt%) did not affect the yield of methyl stearate. Therefore, 6 wt% was chosen as optimum catalyst amount for further reactions. X-SZr catalyst also showed a linear increase in the yield of methyl stearate (41 to 81%) from 1 to 6 wt% catalyst amount which was further increased to 84% with 8 wt% catalyst amount (Fig. 5b) indicating the need of higher catalyst amount as compared to A-SZr.

3.2.4. Kinetic studies with reaction time

The reaction was carried out at various reaction time intervals at 60 °C over 6 wt% catalyst amount. The kinetic profile (Fig. 6) of esterification reaction obtained with time in terms of the consumption of stearic acid (SA) and formation of methyl stearate (MS) showed a fast linear decrease in the concentration of SA up to 30 min; on further increasing the time, decrease in concentration of SA became moderately slow and started to approach saturation after 5 h. An identical trend in the formation of MS was obtained. The initial rates for the consumption of SA (ν) and formation of MS (ν_1) were calculated from the early linear portion of the graph (Fig. 6) from the decreasing concentration of stearic acid and increasing concentration of methyl stearate by using the equations, $\nu = -d[SA]/dt$ and $\nu_1 = d[MS]/dt$, respectively. Both ν and ν_1 rates were found to be almost identical indicating that there is a fine balance between the concentration of the consumption of stearic acid and selective formation of methyl stearate.

By comparing the kinetic profile of both catalysts, A-SZr catalyst showed higher reaction rate (ν) of 0.97 mmol h^{-1} as compared to X-SZr catalyst having lower reaction rate (ν) of 0.66 mmol h^{-1} for the consumption of stearic acid under the similar reaction conditions (Fig. 6). The reaction rate per gram of catalyst (mmol h^{-1} g^{-1}) was also higher for A-SZr (18.94) than X-SZr (12.94). Turnover frequency (TOF, mmol of stearic acid converted per mole of acid site concentration per hour) was calculated for 1 h reaction time and was also found to be significant higher for A-SZr (8.55 h^{-1}) as compared to X-SZr (3.92 h^{-1}).

The results clearly revealed the significant influence of the aerogel structure prepared by SCD technique. The improved structural, textural and acidic properties in terms of higher surface area, pore volume, higher surface to volume ratio and availability of more B and L acid sites in A-SZr catalyst compared to X-SZr catalyst resulted into higher rate of reaction and TOF.

The kinetic investigations were also performed by varying the amount of A-SZr catalyst from 3 to 6 wt% by keeping other reaction conditions and concentration of stearic acid constant. The effect of variation in catalyst amount with respect to formation of methyl stearate is given in Fig. 7a. The pseudo-first order rate constant k (h^{-1}) was determined from the plot of ln[SA] versus time (t) (Fig. 7b), which is a straight line with slope $-k$ and intercept $\ln[SA]_o$ as per the following equation: $\ln[SA] = \ln([SA]_o e^{-kt}) = \ln[SA]_o - kt$

The pseudo-first order rate constant k (h^{-1}) determined at different catalyst amount were: $k \times 10^3$ (wt%) = 3.5 (3), 7.1 (4) and 11.6 (6). These rate constants were also increased in the line of increasing the rates (ν) on increasing the catalyst amount (Fig. 7c) indicating first order dependence on the catalyst amount. The rate constant ($k \times 10^3$) at 6 wt% catalyst amount for A-SZr (11.6 h^{-1}) was also higher than X-SZr catalyst (8.87 h^{-1}). It is also worth to note that the rate of reaction for methyl stearate in the present study over A-SZr catalyst was found to be considerably higher (18.94 mmol h^{-1} g^{-1}) than silica supported tungstophosphoric acid catalyst (~2.3 mmol h^{-1} g^{-1}) [16] for same reaction.

3.3. Reusability of A-SZr catalyst

The activity of re-used A-SZr catalyst showed slight successive decrease (~9%) in the yield of methyl stearate after each cycle till 4th reaction cycle and was stable afterwards (Fig. 8). To recognize the reason of deactivation, the re-used A-SZr catalyst (after 5 reaction cycles) was characterized by FT-IR and elemental sulfur, carbon analysis. The FT-IR spectrum (Fig. S4) of re-used, A-SZr-ru catalyst (washed and dried at 120 °C, 12 h) showed bands at 2850, 2925, 1397, 1461 cm^{-1} which were assigned to the bending/scissoring and stretching vibration of C—H, —CH_2/—CH_3 groups. The FT-IR spectrum of activated, A-SZr-ac catalyst (washed, dried and activated at 600 °C for 2 h in air flow) showed the absence of these bands indicating the removal of organic moieties from the surface of the catalyst during thermal activation. Moreover, considerable decrease in the intensity of band at ~3410 cm^{-1} for surface Zr–OH and S-OH groups associated with the Brönsted acidity of the catalyst was observed, though sulfur bands in the region of 900–1200 cm^{-1} were present in A-SZr-ac catalyst (Fig. S4). The carbon content of fresh and used A-SZr-ac catalyst was found similar (0.03 wt%) indicating no blockage of acid sites by carbon deposition, however, decrease in sulfur content was 50%. Therefore, the slight decrease in the catalyst activity is attributed to the loss of sulfate species leading to a decrease in Brönsted acidity of the catalyst.

4. Comparison of catalytic activity with other heterogeneous and homogeneous catalysts

We have compared the activity of A-SZr catalyst with various other heterogeneous catalysts such as ion-exchange resins, Nafion and montmorillonite K10 as well as homogeneous Brönsted acid namely H_2SO_4 and Lewis acid namely $ZrOCl_2 \cdot 8H_2O$ under similar reaction conditions (Fig. 9). Amberlite IR-120 is a strong acid resin but exhibited very low yield of methyl stearate (44%). The sulfonic ion-exchange resins namely Nafion SAC-13 and Amberlyst-15 catalysts showed 58 and 68% yield, respectively, whereas, montmorillonite K10 clay showed 61% yield. Homogeneous Brönsted acid (H_2SO_4) and Lewis acid ($ZrOCl_2$) resulted slightly higher yield (97%) of methyl stearate than A-SZr (88%); however, use of eco-friendly heterogeneous catalysts is advantageous due to easy separation and re-use of the catalyst. In general, among all the heterogeneous catalysts studied, A-SZr catalyst exhibited higher yields under the similar reaction conditions, which clearly revealed the potential of A-SZr catalyst having both Brönsted and Lewis acid sites.

5. Reaction mechanism

Esterification of stearic acid with methanol may be catalyzed by both Brönsted (H_2SO_4) and Lewis acids ($ZrOCl_2.8H_2O$). However, the initial rate of reaction (ν) was found to be higher (2.15 mmol h^{-1}) in presence of H_2SO_4 as compared to $ZrOCl_2$ catalyst having lower reaction rate (1.58 mmol h^{-1}) for the consumption of stearic acid under the similar reaction conditions. SZr catalyst has both Brönsted (H^+) and Lewis acid sites (Zr^+) as shown in Scheme 3, therefore, both acid sites may take part in the reaction. As rate of Brönsted catalyzed reaction was higher and also the catalyst has higher Brönsted acidity, the studied reaction is supposed to be mainly Brönsted acid catalyzed reaction, wherein H^+ transfers from the Brönsted acid sites of catalyst to carbonyl oxygen of the acid (first step), which is nucleophillic attacked by oxygen of methanol (second step); subsequent deprotonation and loss of water (third step) forms the ester product (left side of Scheme 3).

On the other hand, the Lewis acid sites of SZr catalyst may also take part in the formation of methyl stearate. In the Lewis acid-catalyzed esterification reaction, direct coordination of stearic acid with Lewis Zr^{+} sites is the first step (right side of Scheme 3). In the second and third steps, the reaction followed the same mechanistic step as those of the Brönsted acid catalyzed reaction.

6. Conclusions

Aerogel sulfated zirconia (A-SZr) and xerogel sulfated zirconia (X-SZr) were prepared by sol–gel method followed by supercritical drying (SCD) and conventional thermal drying, respectively. The properties and catalytic activity of both catalysts were compared. The study showed that SCD resulted into the formation of higher surface area and pore volume with ordered porous nano-crystalline structure and more number of accessible Brönsted and Lewis acid sites scattered on larger surface area thus providing higher surface to volume ratio that facilitated the easy diffusion of reactants and product molecules. A-SZr catalyst showed higher reaction rate and TOF under the studied reaction conditions than X-SZr catalyst with pseudo-first order kinetics. Though, re-cycling of A-SZr catalyst showed slight successive decrease in the activity, it exhibited higher activity than other heterogeneous catalysts such as ion exchange resins, nafion and acid K10 clay. In addition, the activity of A-SZr catalyst was comparable with conventional H_2SO_4 (Brönsted) and $ZrOCl_2$ (Lewis) acids indicating its potential to replace the conventional homogeneous Brönsted as well as Lewis acid catalysts owing to having both acid sites.

In conclusion, nano-crystalline aerogel SZr catalyst showed an efficient activity for the esterification of stearic acid with methanol due to the higher mesoporosity, surface area and surface to volume ratio along with good acidic features, which played an important role for the catalytic activity for the studied reaction.

Acknowledgements

CSIR-CSMCRI communication No. 157/2015. Authors are thankful to CSIR Network Programme on Indus Magic (CSC-0123) for financial assistance and to 'Analytical Discipline and Centralized Instrumental Facilities' for providing instrumentation facilities.

Appendix A. Supplementary data

Supplementary data associated with this article can be found, in the online version, at http://dx.doi.org/10.1016/j.apcatb.2016.03.037.

References

[1] F. Ma, M.A. Hanna, Bioresour. Technol. 70 (1999) 1–15.
[2] M. Canakci, J.V. Gerpen, Trans. ASAE 46 (2003) 945–954.
[3] S. Jansri, S.B. Ratanawilai, M.L. Allen, G. Prateepchaikul, Fuel Process. Technol. 92 (2011) 1543–1548.
[4] D.A.G. Aranda, R.T.P. Santos, N.C.O. Tapanes, A.L.D. Ramos, O.A.C. Antunes, Catal. Lett. 122 (2008) 20–25.
[5] E. Lotero, Y. Liu, D.E. Lopez, K. Suwannakarn, D.A. Bruce, J.G. Goodwin Jr., Ind. Eng. Chem. Res. 44 (2005) 5353–5363.
[6] M.M. Gui, K.T. Lee, S. Bhatia, Energy 33 (2008) 1646–1653.
[7] MPOB, Malaysian Oil Palm Statistics 2002, 22nd ed., Malaysian Palm Oil Board, Malaysia, 2003, pp. 56.
[8] F. Chemat, M. Pouxa, S.A. Galema, J. Chem. Soc. Perkin Trans. 2 (1997) 2371–2374.
[9] http://www.chemicalbook.com/ChemicalProductProperty_EN_CB6409834.htm.
[10] J.A. Melero, J. Iglesias, G. Morales, Green Chem. 11 (2009) 1285–1308.
[11] Y.C. Sharma, B. Singh, J. Korstad, Biofuels Bioprod. Bioref. 5 (2011) 69–92.
[12] F. Su, Y. Guo, Green Chem. 16 (2014) 2934–2957.
[13] L. Zatta, E.J.M. Paiva, M.L. Corazza, F. Wypych, L.P. Ramos, Energy Fuels 28 (2014) 5834–5840.
[14] (a) S.B. Neji, M. Trabelsi, M.H. Frikha, Energies 2 (2009) 1107–1117; (b) S.B. Neji, M. Trabelsi, M.H. Frikha, J. Oleo Sci. 60 (2011) 293–299.
[15] (a) W. Liu, P. Yin, X. Liu, W. Chen, H. Chen, C. Liu, R. Qu, Q. Xu, Energy Convers. Manage. 76 (2013) 1009–1014; (b) W. Chen, P. Yin, H. Chen, Z. Wang, Ind. Eng. Chem. Res. 51 (2012) 5402–5407.
[16] C.S. Caetano, I.M. Fonseca, A.M. Ramos, J. Vital, J.E. Castanheiro, Catal. Commun. 9 (2008) 1996–1999.
[17] (a) B.M. Reddy, M.K. Patil, Chem. Rev. 109 (2009) 2185–2208; (b) G.D. J.J. Nair Yadav, Microporous Mesoporous Mater. 33 (1999) 1–48.
[18] M. Hino, S. Kobayashi, K. Arata, J. Am. Chem. Soc. 101 (1979) 6439–6441.
[19] (a) A.A. Kiss, A.C. Dimian, G. Rothenberg, Adv. Synth. Catal. 348 (2006) 75–81; (b) A.A. Kiss, F. Omota, A.C. Dimian, G. Rothenberg, Top. Catal. 40 (2006) 141–150.
[20] M. Hino, S. Takasaki, S. Furuta, H. Matsuhashi, K. Arata, Catal. Commun. 7 (2006) 162–165.
[21] M.L. Grecea, A.C. Dimian, S. Tanase, V. Subbiah, G. Rothenberg, Catal. Sci. Technol. 2 (2012) 1500–1506.
[22] S. Furuta, H. Matsuhashi, K. Arata, Appl. Catal. A 269 (2004) 187–191.
[23] D.E. Lopez, J.G. Goodwin Jr., D.A. Bruce, S. Furuta, App. Catal. A 339 (2008) 76–83.
[24] D. Rattanaphra, A.P. Harvey, A. Thanapimmetha, P. Srinophakun, Fuel 97 (2012) 467–475.
[25] Y. Zhang, W.T. Wong, K.F. Yung, Bioresour. Technol. 147 (2013) 59–64.
[26] M.K. Mishra, B. Tyagi, R.V. Jasra, Ind. Eng. Che. Res. 42 (2003) 5727–5736.
[27] (a) K. Saravanan, B. Tyagi, H.C. Bajaj, Catal. Sci. Technol. 2 (2012) 2512–2520; (b) K. Saravanan, B. Tyagi, H.C. Bajaj, J. Sol-Gel Sci. Technol. 62 (2012) 13–17; (c) K. Saravanan, B. Tyagi, H.C. Bajaj, Ind. J. Chem. 53A (2014) 799–805; (d) K. Saravanan, B. Tyagi, R.S. Shukla, H.C. Bajaj, Fuel 165 (2016) 298–305; (e) K. Saravanan, B. Tyagi, R.S. Shukla, H.C. Bajaj, Appl. Catal. B 172 (2015) 108–115.
[28] (a) B. Tyagi, K. Sidhpuria, B. Shaik, R.V. Jasra, J. Nanosci. Nanotechnol. 6 (2006) 1–10; (b) M.K. Mishra, B. Tyagi, R.V. Jasra, J. Mol. Catal. A 223 (2004) 61–65.
[29] B. Tyagi, C.D. Chudasama, R.V. Jasra, Appl. Clay Sci. 31 (2006) 16–28.
[30] C.A. Emeis, J. Catal. 141 (1993) 347–354.
[31] T. Barzetti, E. Selli, D. Moscotti, L. Forni, J. Chem. Soc. Faraday Trans. 92 (1996) 1401–1407.
[32] J.K. Satyarthi, S. Radhakrishnan, D. Srinivas, Energy Fuels 25 (2011) 4106–4112.
[33] M. Schneider, A. Baiker, Catal. Rev. Sci. Eng. 37 (1995) 515–556.
[34] (a) T. Boiadijieva, G. Cappelletti, S. Ardizzone, S. Rondinini, A. Vertova, Phys. Chem. Chem. Phys. 5 (2003) 1689–1694; (b) C.J. Brodsky, E.I. Ko, J. Non-Cryst. Solids 186 (1995) 88–95; (c) C. Stocker, A. Baiker, J. Non-Cryst. Solids 223 (1998) 165–178.
[35] T. Yamaguchi, T. Jin, K. Tanabe, J. Phys. Chem. 90 (1986) 3148–3152.
[36] S.J. Gregg, K.S.W. Sing, Adsorption, Surface Area and Porosity, 2nd ed., Academic Press, New York, 1982.